panel. The vernier rocket exhaust upon landing may have compacted or blown the upper fluff away nearest the spacecraft.

Subsequent effort was directed toward analyzing the eclipse data, and data from the other Surveyor missions. These results are given in Ref. 7.

References

[1] Lucas, J. W. et al., "Lunar Surface Temperatures and Thermal Characteristics," *Surveyor V Mission Report, Part II: Science Results*, TR 32-1247, 1967, Jet Propulsion Lab., Pasadena, Calif.

[2] Vitkus, G., Lucas, J. W., and Saari, J. M., "Lunar Surface Thermal Characteristics During Eclipse from Surveyors III, V, and after Sunset from Surveyor V," *AIAA Progress in Astronautics and Aeronautics: Thermal Design Principles of Spacecraft and Entry Bodies*, Vol. 21, edited by G. T. Bevans, Academic Press, New York, 1969, pp. 489–505.

[3] Lucas, J. W. et al., "Lunar Surface Temperatures and Thermal Characteristics: Surveyor V Science Results," *Journal of Geophysical Research*, Vol. 73, No. 22, Nov. 15, 1968, pp. 7209–7219.

[4] Jones, B. P., "Density-Depth Model for the Lunar Outermost Layer," *Journal of Geophysical Research*, Vol. 73, No. 24, 1968, pp. 7631–7635.

[5] Winter, D. F. and Saari, J. M., "A New Thermophysical Model of the Lunar Soil," Document DI-82-0725, Boeing Scientific Research Lab., 1968.

[6] Wildey, R. L., Murray, B. C., and Westphal, J. A., "Reconnaissance of Infrared Emission from the Lunar Nighttime Surface," *Journal of Geophysical Research*, Vol. 72, No. 14, 1967, pp. 3743–3749.

[7] Stimpson, L. D. et al., "Revised Lunar Surface Temperatures and Thermal Characteristics from Surveyor," *Analysis of Surveyor Data*, TR 32-1443, 1969, Jet Propulsion Lab., Pasadena, Calif.

NOVEMBER 1970 J. SPACECRAFT VOL. 7, NO. 11

Waffle Plates with Multiple Rib Sizes: I. Stability Analysis

LAWRENCE D. HOFMEISTER*
TRW Systems, Redondo Beach, Calif.

AND

LEWIS P. FELTON†
University of California, Los Angeles, Calif.

A method is presented for the gross buckling analysis of waffle plates having multiple sizes of ribs in each stiffening direction. Rectangular plates having two distinct size ribs arranged in orthogonal and equilateral configurations are investigated in detail. General biaxial in-plane load conditions are considered. The stability criterion is developed by minimizing the total potential energy of the systems. Several examples are presented to illustrate applications of the formulations to plates with discrete ribs, closely spaced ribs, and combinations of the two. Where possible, results are compared to solutions obtained from other sources with good agreement.

Nomenclature

A,Z,I	=	geometric parameters
a,b	=	plate dimensions
c_i,e_j	=	coordinates of orthogonal stiffeners
d	=	primary rib spacing
E_s,E_1,E_2	=	moduli of elasticity of skin, primary, and secondary ribs, respectively
$\bar{e}_x,\bar{e}_y,\bar{e}_{xy}$	=	load eccentricities with respect to middle surface
$\mathbf{F}$	=	vector of generalized forces
$\mathbf{K}$	=	stiffness matrix
L	=	number of displacement functions
N_{1j}	=	critical load
N_x,N_y,N_{xy}	=	applied loads
P_i	=	distributed forces in primary ribs
$\mathbf{S}_x,\mathbf{S}_y,\mathbf{S}_{xy},\mathbf{S}_j$	=	stability matrices
U_{mn},V_{mn},W_{mn}	=	displacement amplitudes
$\mathbf{U}$	=	vector of unknown displacements
h_1,h_2	=	height of primary and secondary ribs, respectively
k_{ij}	=	constants in stress-strain relations
m,n,k	=	integers
t,t_1,t_2	=	thickness of plate skin, primary, and secondary ribs, respectively
$\bar{t}_i,\bar{t}_j$	=	equivalent thickness
u,v,w	=	displacements
Π	=	strain energy
$\alpha_j,\gamma_j,\beta_j$	=	N_x/N_{1j}, N_y/N_{1j}, and N_{xy}/N_{1j}, respectively
ϵ,σ	=	strain and stress, respectively
ν_s	=	Poisson's ratio

Subscripts

s	=	plate skin
$u_{,x},w_{,xx}$	=	$\partial u/\partial x$, $\partial^2 w/\partial x^2$, respectively, etc.

Received August 8, 1969; revision received June 22, 1970. This work was partially supported by Grant NsG-423 from NASA to the late F. R. Shanley, Professor of Engineering, University of California, Los Angeles. The authors wish to acknowledge the fact that the structural concept investigated in this paper originated with him.

* Member of the Technical Staff, formerly Postgraduate Research Engineer, University of Calif., Los Angeles, Calif.

† Assistant Professor of Engineering. Member AIAA.

Introduction

IN a previous paper[1] the behavior and design of integrally stiffened waffle plates having two distinct sizes of orthogonal ribs (see Fig. 1) were investigated for the case of uni-

axial in-plane compressive loads. Such plates are considerably more efficient from a weight standpoint than similarly loaded plates having only one basic size of stiffener and should be competitive with sandwich construction in the range of loading intensity over which the sandwich is normally more efficient. Because such constructions are generally best utilized in biaxial loading fields[2,3] we present herein an analytic method for the computation of the gross buckling loads for two-rib-size waffle plates under biaxial load conditions. The particular cases of orthogonally stiffened (Fig. 1) and equilaterally stiffened (Fig. 2) rectangular plates are examined in detail.

The stability criterion for the plates is developed from expressions for total potential energy. In general, it will be assumed that the smaller (primary) ribs are closely spaced, allowing strain energy expressions for these ribs to be developed by equating their behavior to that of equivalent homogeneous orthotropic plates. The greater spacing of the larger (secondary) ribs makes it necessary to account for their discrete contributions to the total energy of the systems. The prebuckling state is assumed to be linear.

Potential Energy of Stiffened Plates

For a homogeneous continuum in a state of plane stress, an appropriate linear constitutive law may be expressed in the form

$$\begin{Bmatrix}\sigma_x\\ \sigma_y\\ \sigma_{xy}\end{Bmatrix} = \begin{bmatrix}k_{11} & k_{12} & 0\\ k_{12} & k_{22} & 0\\ 0 & 0 & k_{33}\end{bmatrix} \begin{Bmatrix}\epsilon_x\\ \epsilon_y\\ \epsilon_{xy}\end{Bmatrix} \tag{1}$$

The strain energy is then given by

$$\Pi = \tfrac{1}{2}\int_V(\sigma_x\epsilon_x + \sigma_y\epsilon_y + \sigma_{xy}\epsilon_{xy})dV \tag{2}$$

Considering a rectangular plate of dimensions a and b (Fig. 1), linear strain-displacement relations and the Kirchoff hypothesis lead to

$$\epsilon_x = u_{,x} + zw_{,xx},\ \epsilon_y = v_{,y} + zw_{,yy} \tag{3a}$$

$$\epsilon_{xy} = u_{,y} + v_{,x} + 2zw_{,xy} \tag{3b}$$

where ϵ is strain, and u, v, and w are plate displacements in the x, y, and z coordinate directions, respectively.

Substituting Eqs. (1) and (3) into Eq. (2), and integrating over z gives

$$\Pi = \frac{1}{2}A\int_0^a\int_0^b [k_{11}u_{,x}^2 + 2k_{12}u_{,x}v_{,y} + k_{22}v_{,y}^2 + k_{33}(u_{,y} + v_{,x})^2]dydx + \frac{1}{2}AZ\int_0^a\int_0^b [k_{11}u_{,x}w_{,xx} + k_{12}(v_{,y}w_{,xx} + u_{,x}w_{,yy}) + k_{22}v_{,y}w_{,yy} + 2k_{33}w_{,xy}(u_{,y} + v_{,x})]dydx + \frac{1}{2}AI\int_0^a\int_0^b (k_{11}w_{,xx}^2 + k_{22}w_{,yy}^2 + 2k_{12}w_{,xx}w_{,yy} + 4k_{33}w_{,xy}^2)dydx \tag{4}$$

The terms A, Z, and I are constants obtained in the integration, and will be given more explicit definitions in the following sections. Equation (4) can now be specialized to treat various components of the multiply stiffened plate.

For the *plate skin* of uniform thickness t, the coefficients in Eq. (1) reduce to

$$k_{11} = k_{22} = E_s/(1 - \nu_s^2) \tag{5a}$$

$$k_{12} = E_s\nu_s/(1 - \nu_s^2) = \nu_s k_{11} \tag{5b}$$

$$k_{33} = E_s/2(1 + \nu_s) \tag{5c}$$

Using these, and using $A = t$, $Z = 0$, and $I = t^3/12$ in Eq. (4), we obtain the *strain energy for the plate skin*, Π_s.

Considering the closely spaced primary ribs to behave in a manner analogous to homogeneous orthotropic sheets, Meyer[4]

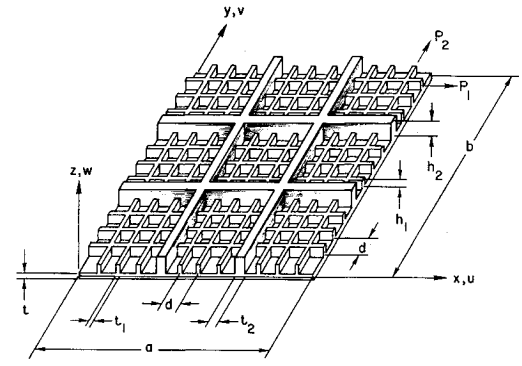

Fig. 1 Waffle plate with two sizes of orthogonal ribs.

has shown that the stress-strain equations for the stiffening system are similar in form to Eqs. (1). Relations of this type may be extended to apply to any regular stiffening arrangement provided the rib spacing is small with respect to the overall plate dimensions. For the primary ribs, integration of the strain energy over z gives

$$A = h_1,\quad Z = h_1 + t,\qquad I = \tfrac{1}{3}h_1^2 + \tfrac{1}{2}h_1t + \tfrac{1}{4}t^2 \tag{6}$$

where h_1 is the height of the ribs as measured from the top surface of the plate skin.

For *orthogonal primary ribs* (Fig. 1), with the quantities P_1 (x direction) and P_2 (y direction) denoting forces per unit height uniformly distributed in the ribs, it follows that primary rib strains and stresses are

$$\epsilon_x = P_1/E_1t_1,\quad \epsilon_y = P_2/E_1t_1 \tag{7}$$

$$\sigma_x = P_1/d,\quad \sigma_y = P_2/d,\quad \sigma_{xy} = \sigma_{yx} = 0 \tag{8}$$

Combining Eqs. (7) and (8) by eliminating P_1 and P_2 gives constitutive relations having the form of Eq. (1) with

$$k_{11} = k_{22} = E_1t_1/d,\quad k_{12} = k_{33} = 0 \tag{9}$$

Substituting Eqs. (9) and (6) in Eq. (4) then gives the strain energy for the *orthogonal primary stiffening arrangement*, Π_1.

If there are no ribs parallel to the x axis, then Eqs. (1) still apply with $k_{11} = 0$. Similarly, for no stiffeners in the y direction, $k_{22} = 0$.

For *three-way equilateral primary ribs* (Fig. 2) proceeding as in the previous case, it follows that

$$k_{11} = k_{22} = 3^{3/2}E_1t_1/4d \tag{10a}$$

$$k_{33} = k_{12} = 3^{1/2}E_1t_1/4d \tag{10b}$$

For *secondary ribs* with a spacing of the same order of magnitude as the plate dimensions, we must account for the discrete contributions of each secondary rib. For an *orthogonal*

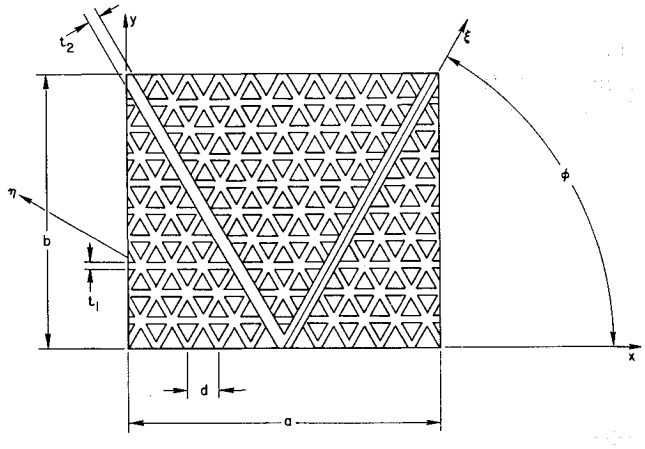

Fig. 2 Waffle plate with two sizes of equilateral ribs.

secondary rib oriented parallel to the x direction (Fig. 1),

$$\sigma_x = E_2\epsilon_x \tag{11}$$

Therefore,

$$k_{11} = E_2, \quad k_{22} = k_{12} = k_{33} = 0 \tag{12}$$

Using Eq. (12) in Eq. (4), and noting that integration over y gives a value of t_2 only at $y = c_i$, where c_i is the rib location from the y axis, we obtain

$$\Pi_2 = A\frac{E_2t_2}{2}\int_0^a (u,^2_x)_{y=ci}\,dx + \frac{AZE_2t_2}{2}\int_0^a (u_{,x}w_{,xx})_{y=ci}\,dx + \frac{AIE_2t_2}{2}\int_0^a (w,^2_{xx})_{y=ci}\,dx \tag{13a}$$

where

$$A = h_2, \quad Z = h_2 + t \tag{13b}$$

$$I = \tfrac{1}{3}h_2^2 + \tfrac{1}{2}h_2t + \tfrac{1}{4}t^2 \tag{13c}$$

By a similar derivation, Π_2 for an orthogonal secondary rib oriented parallel to the y direction at a distance $x = e_j$ can be obtained. The total strain energy for all orthogonal secondary ribs is obtained by summing the contributions of individual stiffeners.

For *three-way secondary ribs*, integration of strain energy expressions for generalized configurations would be complicated and computationally time consuming. For this reason, the subsequent developments for three-way stiffening systems are restricted to square plates having the particular secondary rib arrangement shown in Fig. 2. Because the two secondary ribs in Fig. 2 extend from the midpoint of one edge to the opposite corners of a square plate, the angle ϕ is 63.5° rather than the 60° assumed for the primary ribs. In terms of the ξ,η coordinate system, it follows that the strain energy for the secondary rib located where $\eta = 0$ is

$$\Pi_2 = AE_2t_2\int_0^{5^{1/2}a/2} (u,^*_\xi)^2_{\eta=0}\,d\xi + AZE_2t_2\int_0^{5^{1/2}a/2} [(w,^*_{\xi\xi})^2_{\eta=0}]\,d\xi + AIE_2t_2\int_0^{5^{1/2}a/2} (u,^*_\xi w,^*_{\xi\xi})_{\eta=0}\,d\xi \tag{14}$$

where u^* is the axial displacement of the rib, and w^* is the displacement in the z direction at the rib location. Expressions for A, t, and I are given in Eqs. (13).

As the plate and primary stiffeners deflect, the *applied in-plane external loads do work* Π_L, where[5]

$$\Pi_L = \int_0^a\int_0^b \left[N_x\left(u_{,x} + \frac{1}{2}w,^2_x + \bar{e}_xw_{,xx}\right) + N_y\left(v_{,y} + \frac{1}{2}w,^2_y + \bar{e}_yw_{,yy}\right) + N_{xy}(u_{,y} + v_{,x} + w_{,x}w_{,y} + 2\bar{e}_{xy}w_{,xy})\right]dydx \tag{15}$$

Here, N_x and N_y are the in-plane forces per unit length in the x and y directions, respectively, positive in compression, and N_{xy} is the in-plane shear. The $\bar{e}$'s are the eccentricities of the loads from the reference (middle) surface.

Again, the discrete work done by the external load during bending of the secondary ribs must be considered separately. For *orthogonal* secondary ribs in both the x and y directions, this work is given by

$$\Pi_{L_2} = \frac{1}{2}\sum_j\left(\frac{h_2t_2}{\bar{t}_j}\right)\int_0^b N_y(w_{,y})^2_{x=ej}\,dy + \frac{1}{2}\sum_i\left(\frac{h_2t_2}{\bar{t}_i}\right)\int_0^a N_x(w_{,x})^2_{y=ci}\,dx \tag{16}$$

where $\bar{t}_j$ is the equivalent thickness of the plate over which N_y acts, and $\bar{t}_i$ the equivalent thickness over which N_x acts.

The work done by the applied loads on the displacements as the *three-way* secondary stiffeners of Fig. 2 deflect is

$$\Pi_{L_2} = \left(\frac{h_2t_2}{\bar{t}_j}\right)\int_0^{5^{1/2}a/2} N_y(w,^*_\xi)^2_{\eta=0}\,d\xi + \left(\frac{h_2t_2}{\bar{t}_i}\right)\int_0^{5^{1/2}a/2} N_x(w,^*_\xi)^2_{\eta=0}\,d\xi \tag{17}$$

The *total potential energy* of the stiffened plate system is

$$\Pi = \Pi_s + \Pi_1 + \Pi_2 - (\Pi_L + \Pi_{L_2}) \tag{18}$$

The Theorem of Minimum Potential Energy[6] states that among all the compatible displacements fields which satisfy the geometric boundary conditions, that displacement field which makes the potential energy an absolute minimum satisfies the equilibrium conditions of the structural system. This theorem can be used to deduce differential equations of equilibrium (Euler Equations) and associated boundary conditions (Transversality Conditions). These equations can then, in theory, be solved for the displacement field of the loaded stiffened plate. Alternatively, the theorem can be used as a starting point for a numerical solution. For example, the finite element method[7] could be used to find the buckling loads of the stiffened plates. However, this would lead to large eigenvalue problems.

The method to be developed in the next section was selected in order to avoid large systems of equations. It closely parallels the classical Rayleigh-Ritz procedure[8] in that the approximate displacement functions chosen for numerical minimization of Eq. (18) satisfy explicitly the boundary conditions and apply to the stiffened plate system as a whole.

Stability Analysis of Plates with Simply Supported Edges

Let us derive explicit formulas for the various energy expressions by assuming the stiffened plate has simply supported edges and then use these expressions to deduce the stability criterion. The following displacement functions satisfy the conditions of simply supported edges for the rectangular plate.

$$u = \sum_{m=1}^{L}\sum_{n=1}^{L} U_{mn}\sin\frac{m\pi y}{b}\cos\frac{n\pi x}{a} \tag{19a}$$

$$v = \sum_{m=1}^{L}\sum_{n=1}^{L} V_{mn}\cos\frac{m\pi y}{b}\sin\frac{n\pi x}{a} \tag{19b}$$

$$w = \sum_{m=1}^{L}\sum_{n=1}^{L} W_{mn}\sin\frac{m\pi y}{b}\sin\frac{n\pi x}{a} \tag{19c}$$

where m and n are integers, and U_{mn}, V_{mn}, and W_{mn} are unknown displacement amplitudes; L independent functions are considered in each coordinate direction. Using Eqs. (19) in (4), and performing the integrations gives

$$\Pi = \frac{ab\pi^2}{8}A\sum_m\sum_n\{k_{11}U_{mn}^2(n/a)^2 + k_{22}V_{mn}^2(m/b)^2 + 2k_{12}U_{mn}V_{mn}(n/a)(m/b) + k_{33}[U_{mn}(m/b) + V_{mn}(n/a)]^2\} + \frac{ab\pi^3}{8}AZ\sum_m\sum_n W_{mn}\{k_{11}U_{mn}(n/a)^3 + k_{33}V_{mn}(m/b)^3 + (k_{11} + 2k_{33})(m/b)(n/a)[V_{mn}(n/a) + U_{mn}(m/b)]\} + \frac{ab\pi^4}{8}AI\sum_m\sum_n W_{mn}^2[k_{11}(n/a)^4 + k_{22}(m/b)^4 + 2(k_{11} + 2k_{33})(m/b)^2(n/a)^2] \tag{20}$$

This expression can now be specialized to give the strain energy of the plate skin or primary ribs by using the appropriate coefficients k_{ij}. The integration leading to Eq. (20) is par-

Table 1 Critical buckling loads for plates with one secondary rib only ($E_s = E_2 = 10.5 \times 10^6$ psi, $\nu_s = 0.313$, $a = b = 12.0$ in., $t = 0.1$ in.)

Case (Fig. 3)	t_2, in.	h_2, in.	Cycles of iteration (Ref. 11)	$(N_x)_{cr}$ (klb/in.) Present study	Ref. 12
a	0.228	0.527	4	1.06	1.17
b	0.322	0.373	5	0.749	0.814
c	0.322	0.373	2	0.416	0.582

ticularly simple due to the orthogonality of the sine and cosine functions in the assumed displacements.

The substitution of the displacement functions in Eq. (4), or alternatively in Eq. (13a), to compute Π_2 must be considered carefully, since the displacements are evaluated at specific locations on the plate, namely at $y = c_i$. After this substitution, the integration for the secondary ribs parallel to the x axis gives, for example,

$$\Pi_2 = \frac{a\pi^2}{4} AE_2t_2 \sum_k \sum_m \sum_n \left(\frac{n}{a}\right)^2 \Big[U_{mn}U_{kn} + ZU_{mn} \times W_{kn}\frac{n\pi}{a} + IW_{mn}W_{kn}\left(\frac{n\pi}{a}\right)^2 \Big] \sin\frac{m\pi c_i}{b} \sin\frac{k\pi c_i}{b} \quad (21)$$

The strain energy for the ribs parallel to the y axis can be similarly computed.

As noted previously, in order to render an analysis of the three-way stiffening system tractable, consideration is limited to the particular secondary stiffener configuration shown in Fig. 2, in which $a = b$. Referring again to the ξ,η coordinate system, it follows that the deflections of the secondary rib are

$$u^*(\xi) = \sum_{m=1}^{L} \sum_{n=1}^{L} \Big[U_{mn}\frac{1}{5^{1/2}} \sin\frac{n\pi\xi}{5^{1/2}a} \sin\frac{2m\pi\xi}{5^{1/2}a} + V_{mn}\frac{2}{5^{1/2}} \cos\frac{n\pi\xi}{5^{1/2}a} \cos\frac{2m\pi\xi}{5^{1/2}a} \Big] \quad (22a)$$

$$w^*(\xi) = \sum_{m=1}^{L} \sum_{n=1}^{L} W_{mn} \cos\frac{n\pi\xi}{5^{1/2}a} \sin\frac{2m\pi\xi}{5^{1/2}a} \quad (22b)$$

As a consequence of having chosen the particular rib configuration shown in Fig. 2, all arguments of the sine and cosine functions in Eqs. (22), are integer multiples of each other. This considerably simplifies the integration to deduce the strain energy. Substituting Eqs. (22) in (14) and integrating, we obtain

$$\Pi_2 = \frac{2(5^{1/2})\pi^2}{100a} AE_2t_2 \sum_{m=1}^{L} \sum_{n=1}^{L} [U_{mn}^2(4m^2 + n^2) + 4V_{mn}^2(4m^2 + n^2) - 8U_{mn}V_{mn}] + \frac{2(5^{1/2})\pi^3}{100a^2} AZE_2t_2 \sum_{m=1}^{L} \sum_{n=1}^{L} \{W_{mn}V_{mn}[4mn^2 + 4m(n^2 + 4m^2)] - W_{mn}U_{mn}[4m^2n + n(n^2 + 4m^2)]\} + \frac{2(5^{1/2})\pi^4}{100a^3} AIE_2t_2 \sum_{m=1}^{L} \sum_{n=1}^{L} W_{mn}^2[(n^2 + 4m^2)^2 + 4m^2n^2] \quad (23)$$

By following procedures similar to those used in the development of Eqs. (20–23), the work done by applied loads may be expressed in terms of displacement amplitudes. These operations are fairly straightforward, and the resulting equations will not be included here.

Stability Criterion

After all the integrations have been carried out, the total potential energy given by Eq. (18) becomes a function of the arbitrary displacement amplitudes

$$\Pi = \Pi(U_{11},U_{12},\ldots,U_{LL},V_{11},V_{12},\ldots,V_{LL},W_{11},\ldots,W_{LL}) \quad (24)$$

The requirement that the potential energy must be minimized can be stated as

$$\delta\Pi = 0 = (\partial\Pi/\partial U_{11})\delta U_{11} + \ldots + (\partial\Pi/\partial W_{LL})\delta W_{LL} \quad (25)$$

Since the variations of the displacement amplitudes are independent, the above stationary principle generates a system of $3L^2$ linear algebraic equations of form

$$\begin{aligned} \partial\Pi/\partial U_{11} &= 0 \\ &\cdot \\ &\cdot \\ \partial\Pi/\partial W_{LL} &= 0 \end{aligned} \quad (26)$$

Applying the above reasoning to Eq. (18) leads to a system of simultaneous equations with the displacement amplitudes as unknown. This system of equations may be expressed by

$$(\mathbf{K} - N_x\mathbf{S}_x - N_y\mathbf{S}_y - N_{xy}\mathbf{S}_{xy})\mathbf{U} = \mathbf{F} \quad (27)$$

In this equation $\mathbf{U}$ is a vector of the unknown displacement amplitudes U_{mn}, V_{mn}, and W_{mn}, where m and n each assume all values from 1 to L, and $\mathbf{F}$ is a vector of generalized forces.[9] $\mathbf{K}$ is a $3L^2$ by $3L^2$ system stiffness matrix in the $\mathbf{U}$ generalized coordinates and the $\mathbf{S}_x$, $\mathbf{S}_y$, and $\mathbf{S}_{xy}$, also $3L^2$ by $3L^2$, are the stability matrices[10] in the $\mathbf{U}$ coordinates.

Now, defining $\alpha_j = N_x/N_{ij}$, $\gamma_j = N_y/N_{1j}$, and $\beta_j = N_{xy}/N_{1j}$, Eq. (27) may be put in the form

$$(\mathbf{K} - N_{1j}\mathbf{S}_j)\mathbf{U} = \mathbf{F} \quad (28)$$

where the term

$$\mathbf{S}_j = \alpha_j\mathbf{S}_x + \gamma_j\mathbf{S}_y + \beta_j\mathbf{S}_{xy} \quad (29)$$

defines the combined stability matrix for independent load condition j. The parameters α_j, β_j, and γ_j are ratios of the various loads applied in loading condition j and are specified before the analysis is started. After N_{1j} has been calculated, N_x, N_y, and N_{xy} can be computed from α_j, γ_j, and β_j.

The stability criterion can be developed from Eq. (28) by considering that the amplitude functions $\mathbf{U}$ grow without bounds as the plate becomes unstable. This occurs when the value of N_{1j} is such that the determinant of the matrix $(\mathbf{K} - N_{1j}\mathbf{S}_j)$ becomes zero. Finding the critical buckling load N_{1j} for this condition is identical to solving the eigenvalue problem[8]

$$(\mathbf{K} - N_{1j}\mathbf{S}_j)\mathbf{U} = 0 \quad (30)$$

Solution for the lowest critical load N_{1j} was achieved in this work by using an iteration scheme employing matrix decomposition.[11]

Examples

A program was written in FORTRAN IV for an IBM 360/75 computer to assemble the system stiffness and stability matrices of Eq. 30, and to solve the eigenvalue problem. Several examples are presented here, and, where possible, results are compared to solutions obtained from other sources.

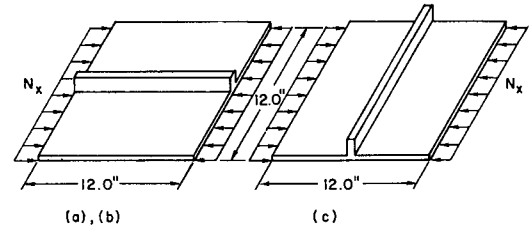

Fig. 3 Example 1 configurations (see Table 1).

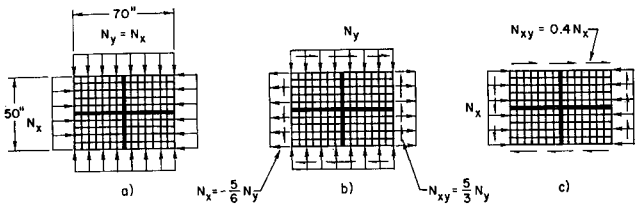

Fig. 4 Example 3 (schematic; ribs denoted by lines; see Table 3).

Example 1. Plates with One Secondary Rib Only

For plates stiffened by ribs spaced at intervals not allowing their effects to be "smeared out," Timoshenko[12] presents solutions based on consideration of bending energy only. In order to compare with these results, U_{mn} and V_{mn} are set equal to zero for all m and n, eliminating stretching energy in the preceding derivation.

Three simply supported square plates subjected to uniaxial compression ($\alpha = 1.0$, $\gamma = \beta, = 0$) were considered, as shown in Fig. 3. Cases a and b are plates with a single centrally located rib oriented parallel to the load direction. The rib of case a is much stiffer than the rib of case b. The plate of case c has the rib oriented transverse to the load direction.

Plate properties, rib dimensions, and results are shown in Table 1. Results for critical buckling loads are seen to be in good agreement with those of Ref. 12 but are slightly lower because the work of Ref. 12 uses only three different mode shapes, while we use 25 displacement shapes ($L = 5$). Using fewer shapes causes the buckling pattern to be somewhat constrained and the critical load correspondingly higher.

Example 2. Plates with Closely Spaced (Primary) Ribs

Results for three cases of uniaxially loaded square plates are shown in Table 2. The first two cases are plates with unidirectional stiffeners oriented in the x and y directions, respectively. The third case is an orthogonally stiffened plate similar to that of Fig. 1, but without the secondary ribs. All plates are assumed to be loaded by distributed forces N_x. Dimensions and material properties shown in Table 2 are taken from Ref. 5.

All cases were solved both with and without consideration of stretching, and results are compared to solutions presented in Ref. 5. Agreement with Ref. 5 is good when stretching and bending are both considered but is less satisfactory when stretching is neglected. For this reason, all the subsequent examples containing closely spaced ribs consider both bending and stretching.

With the effect of the primary stiffeners averaged out over the plate area, the buckling mode of the plate can be represented accurately for simple loading cases by only one mode shape ($L = 1$), as in classical plate buckling theory. That is, the potential energy can be minimized by considering only one term in each of Eqs. (19), instead of a superposition of sine and cosine terms. The resulting stiffness and stability

Table 2 Critical buckling loads for plates with primary stiffeners only ($E_s = E_1 = 10.5 \times 10^6$ psi, $\nu_s = 0.3$, $a = b = 23.75$ in., $t = 0.028$ in., $t_1 = 0.096$ in., $h_1 = 0.302$ in., $d = 1.0$ in.)

Case	$(N_x)_{cr}$ (klb/in.)		
	Ref. 5	No stretching	With stretching
a) One-way, x direction	0.125	0.188	0.119
b) One-way, y direction	0.023	0.002	0.022
c) Two-way	0.294	0.376	0.281

Table 3 Critical buckling loads for plates with primary and secondary orthogonal stiffening ($E_s = E_1 = E_2 = 30 \times 10^6$ psi, $\nu_s = 0.283$, $a = 70.0$ in., $b = 50.0$ in., $t = 0.0423$ in., $d = 3.544$ in., $t_1 = 0.5226$ in., $h_1 = 0.4577$ in., $t_2 = 0.7500$ in., $h_2 = 1.000$ in.)

Case (Fig. 4)	Critical combined loads (klb/in.)		
	N_x	N_y	N_{xy}
a	0.6834	0.6834	0.0
b	−0.8646	1.0375	1.7292
c	1.7509	0.0	0.7004

matrices are of order 3, and closed-form expressions can be deduced for computation of the critical buckling load. It should also be noted that using only one mode shape will lead to a good approximation of the critical load in the case of plates having both primary and secondary stiffeners.

In the aforementioned scheme, ranges of n and m values were considered, and those which gave the lowest value of N_{1j} were taken to constitute the solution. That is, even though a superposition of mode shapes was not used, many individual mode shapes were tried independently to minimize the potential energy expression for the stiffened plate.

For simple loadings, such as uniaxial or biaxial compression, only one shape function for each independent displacement was necessary, as discussed above, to compute the failure load. For combined loads and shear, as in the following examples, a superposition of mode shapes was found to be required.

Example 3. Plates with Primary and Secondary Orthogonal Ribs

A rectangular plate, 70 × 50 in., stiffened with closely spaced orthogonal primary ribs and a single centrally located secondary rib in each coordinate direction, was analyzed for the three distinct loading conditions shown in Fig. 4. The loading ratios for each case are maintained by selecting values of α, γ, and β; e.g., for case b, $\alpha = -\frac{5}{6}$, $\gamma = 1.0$, and $\beta = \frac{5}{8}$. Computed critical loads are shown in Table 3. Analysis of the resulting eigenvectors indicates that the first fundamental mode dominates in all cases. However, for case b, the second mode enters significantly into the shape, while for case c, the mode for which $m = 2$, $n = 1$ is also significant. Computation time was on the order of 0.03 sec.

Example 4. Plates with Primary and Secondary Three-Way Stiffening

As a final example, the configuration shown in Fig. 2 was analyzed for a case of equal biaxial compression. Plate properties were taken as $E_s = E_1 = E_2 = 10.5 \times 10^6$ psi, $\nu_s = 0.313$, $a = b = 12.0$ in., $t = 0.047$ in., $d = 1.818$ in., $t_1 = 0.053$ in., $h_1 = 0.574$ in., $t_2 = 0.150$ in., and $h_2 = 1.00$ in. In Eqs. (19), L was chosen equal to 3.

Analysis indicates that the critical load is given by $N_x = N_y = 4.7726$ klb/in. Components of all nine displacement functions are significant in the final result.

In conclusion, the procedures described herein may be used in conjunction with synthesis algorithms for future studies of the efficiency of this structural concept.

References

[1] Hofmeister, L. D. and Felton, L. P., "Synthesis of Waffle Plates with Multiple Rib Sizes," *AIAA Journal*, Vol. 7, No. 12, Dec. 1969, pp. 2193–2199.

[2] Dow, N. F., Levin, L. R., and Troutman, J. L., "Elastic Buckling Under Combined Stresses of Flat Plates with Integral Waffle-Like Stiffening," TN 3059, Jan. 1954, NACA.

[3] Schmit, L. A. and Kicher, T. P., "Structural Synthesis of Symmetric Waffle Plate," TN D-1691, Dec. 1962, NASA.

[4] Meyer, R. R., "Buckling of 45° Eccentric-Stiffened Waffle Cylinders," *Journal of the Royal Aeronautical Society*, Vol. 71, No. 679, July 1967, pp. 516–520.

[5] McElman, J. A., Mikulas, M. M., and Stein, M., "Static and Dynamic Effects of Eccentric Stiffening of Plates and Cylindrical Shells," *AIAA Journal*, Vol. 4, No. 5, May 1966, pp. 887–894.

[6] Wang, C. T., *Applied Elasticity*, McGraw-Hill, New York, 1953.

[7] Zienkiewicz, O. C. and Cheung, Y. K., *The Finite Element Method in Structural and Continuum Mechanics*, McGraw-Hill, London, 1967.

[8] Hurty, W. C. and Rubinstein, M. F., *Dynamics of Structures*, Prentice-Hall, Englewood Cliffs, N. J., 1965.

[9] Rubinstein, M. F., *Matrix Computer Analysis of Structures*, Prentice-Hall, Englewood Cliffs, N. J., 1967.

[10] Kapur, K. K. and Hartz, B. J., "Stability of Plates Using the Finite Element Method," *Journal of the Engineering Mechanics Division*, ASCE, Vol. 92, No. EM2, April 1966, pp. 177–195.

[11] Rubinstein, M. F. and Rosen, R. R., "Dynamic Analysis by Matrix Decomposition," *Journal of the Engineering Mechanics Division*, American Society of Civil Engineers, Vol. 94, No. EM2, April 1968, pp. 385–395.

[12] Timoshenko, S. P. and Gere, J. M., *Theory of Elastic Stability*, 2nd ed., McGraw-Hill, New York, 1961.

NOVEMBER 1970 J. SPACECRAFT VOL. 7, NO. 11

Waffle Plates with Multiple Rib Sizes: II. Design Examples

LAWRENCE D. HOFMEISTER*
TRW Systems, Redondo Beach, Calif.

AND

LEWIS P. FELTON†
University of California, Los Angeles, Calif.

The efficiency of minimum-weight designs of waffle plates having two rib sizes in each stiffening direction is investigated. A wide variety of configurations are examined, including orthogonal and three-way stiffening patterns. Formulations allow multiple independent general in-plane loads. The design problem is expressed as an inequality-constrained minimization problem, and solved using an interior penalty function optimization algorithm. Designs for plates with only one level of stiffeners agree favorably with results of other studies. For these same examples, incorporation of a second rib size is shown to result in major reductions in required weight. Detailed studies of square plates under uniaxial and equal biaxial loads show that waffle plates with two sizes of ribs compare more favorably to sandwich plates than those with a single stiffener size.

Nomenclature

a,b	=	plate length in the x and y directions, respectively
C	=	constant
D	=	$Et^3/12\ (1 - \nu^2)$ = skin bending stiffness
d	=	spacing of primary (smaller) ribs in x direction
d_x,d_y	=	spacings of secondary (larger) ribs
E	=	Young's modulus
$g_i(\mathbf{X})$	=	constraints
h_1,h_2	=	height of primary and secondary ribs, respectively
$N_i(\mathbf{X})$	=	critical loads
N	=	applied load
$Q(\mathbf{X},\mathbf{X})^{(k)}$	=	penalty function
t	=	skin thickness
t_1,t_2	=	thickness of primary and secondary ribs, respectively
u,v,w	=	plate displacements in x, y, and z directions, respectively
$W(\mathbf{X})$	=	plate weight
$\mathbf{X}$	=	vector of design variables
ν	=	Poisson's ratio
ρ	=	material density
σ	=	stress
σ_y	=	yield stress

Received June 22, 1970. This work was partially supported by Grant NsG-423 from NASA to the late F. R. Shanley, Professor of Engineering, University of California, Los Angeles. The authors wish to acknowledge the fact that the structural concept investigated in this paper originated with him.

* Member of the Technical Staff; formerly Postgraduate Research Engineer, University of Calif., Los Angeles, Calif.

† Assistant Professor of Engineering. Member AIAA.

Introduction

RESULTS of an initial study showing the favorable relative efficiencies of waffle plates with multiple sizes of stiffening ribs have been previously reported.[1] This initial study was confined to uniaxially loaded plates containing orthogonal stiffening patterns of the types illustrated schematically in Figs. 1g–j.

The stability analysis formulated in Ref. 1 has been subsequently extended and refined[2] to accommodate general biaxial loading conditions, coupled plate bending and stretching, and equilateral stiffening configurations of the types shown in Figs. 1c and 1k. This improved formulation makes possible more extensive investigation of the efficiency of the multiple-rib-size concept, the results of which are detailed herein.

Design Problem

In this investigation, the minimum-weight design of simply supported rectangular plates having two "levels" of stiffeners and subjected to multiple independent in-plane loads will be considered. Behavior will be assumed to be elastic, with limitations imposed by the possibility of buckling below or at the yield stress σ_y. Modulus of elasticity E, Poisson's ratio ν, material density ρ, plate dimensions a and b, and magnitudes and directions of the applied loads will be assumed to be specified. In each case, the primary (smaller) ribs will also be assumed to have identical size and spacing in all orientations. In addition, spacing and location of secondary (larger) ribs will be specified, and the effect of variation of these parameters on the final designs will be determined parametrically.